RSC Advances

ROYAL SOCIETY OF CHEMISTRY

www.rsc.org/advances

This article highlights the design considerations for the development of robust and durable bio-inspired synthetic adhesives.

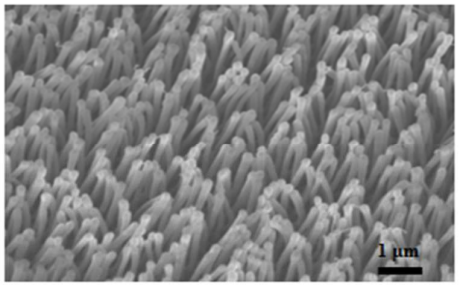

A State-of-the-Art Review and Analysis on the Design of Dry Adhesion Materials for Applications such as Climbing Micro-robots

Rahul Sahay, Hong Yee Low[1], Avinash Baji[2], Shaohui Foong, Kristin L. Wood

Engineering Product Development (EPD) Pillar,
Singapore University of Technology and Design (SUTD),
8 Somapah Rd,
Singapore 487372, Singapore

Abstract

Miniaturization of robotic systems have led to a demand for an alternative adhesive as footpad of robots, with primary requirements of minimizing energy expenditure and satisfying performance and operational scenarios such as surveillance and reconnaissance in multi-sort structures. Inspired by nature, the dry adhesive concept as seen in climbing insects such as the gecko has drawn significant interest from researchers. Adhesion in geckos is attributed to micro/nano fibrils found on its feet that rely on van der Waals forces to adhere to a surface, hence the terminology of dry adhesive. While immense progress has been made in the design and fabrication of multiscale hierarchical adhesive structures, the robustness, durability and endurance (ability to adhere to surfaces for an extended period of time) of gecko-foot mimetic dry adhesive still lags behind their biological counterparts. In this review article, we highlight the design considerations for the development of robust and durable bio-inspired synthetic adhesives. Current challenges and future directions are also highlighted for the design and development of robust and durable dry adhesive structures.

[1] Corresponding author: Tel: +65-6499 4612
Email: hongyee_low@sutd.edu.sg
[2] Corresponding author: Tel: +65 6499 4502; Fax: +65 6779 5161
Email: avinash_baji@sutd.edu.sg

Keywords: dry-adhesives; durability; adhesive forces; gecko; robustness; materials design; micro-robotics

1. Introduction

Climbing is a capability that robotic researchers have been intensely pursuing in the last decade.[1-3] A promising approach useful for climbing is based on dry-adhesion that is inspired by the Gecko, which is arguably nature's most prominent and agile smooth surface climber. While there are many competing methods and techniques, such as vacuum/air suction[4] and magnetic phenomena/attraction[5], to provide an active force to maintain continuous contact with the vertical surface, adhesion-based approach has certain advantages that make it highly suited for a number of applications , including climbing robotics and transformer applications[6-11]. Some of the advantages include lightweight, compact and very low power consumption during operation. These factors are especially crucial for the performance and capabilities of a climbing robot. There are a number of highly successful climbing robots (including the stickybot[1]) using directional adhesion which have illustrated the capability of using adhesive force as a means to provide elementary climbing locomotion; however, there have not been sufficient analysis on the durability of the adhesive, ability to attach and detach repeatedly and ability to maintain extended period of adhesion. Addressing these issues will introduce a new dimension to the capabilities of climbing robots to allow them to maintain a vertical/upside down state for extended periods of time for a wide variety of applications.

Various biological species such as beetles, spiders and geckos have hairy limbs that allow them to cling on to wide variety of surfaces[12-15]. The adhesion in these biological species is attributed to hair like fibrillar structures that are capable of adhering to surfaces by relying on surface contact forces such as van der Waals (vdW) forces.[16, 17] In the case of geckos, each toe

on its feet consists of lamellae structures (meso scale) that are composed of dense, hair like fibrils called setae (micro scale). Each setae is further branched into numerous spatula (nano scale)[18]. Figure 1 illustrates the hierarchical setae-spatula structures. Its strong adhesion system is attributed to the hierarchical architecture of the fibrillar structure that has microscale setae which splits into multiple nanosized spatulas thereby increasing the vdW force by compiling the force created by each spatula. Contact splitting and hierarchical design increases the effective compliance of the micro/nano fibrillar structure and also enables equal load sharing helping the structure achieve optimum adhesion. This dry-adhesion has encouraged materials scientists and engineers to develop bio-inspired synthetic dry adhesives based on carbon nanotubes[19, 20], polymer pillars[21, 22] and elastomers[23].

In general, the applications for bio-mimetic adhesive can be categorized into (1) a static adhesive pad and (2) a dynamic adhesive pad. In this article, we define a static adhesive pad as a stand-alone feature, tape or film, such as adhesive plasters, used for coupling of an artefact to a surface without subsequent motion, and a dynamic adhesive pad as integrated feature, tape, or film, which is used in conjunction with the movement of a device such as micro-robots. Important criteria for a dynamic adhesive pad are robustness, durability, endurance, minimal energy usage as well as reusability, reversibility and substrate tolerance [24]. Each of these criteria is appropriately defined and described in the subsequent sections of the review.

In nature, the biological species cleverly exploit dynamic adhesion to maintain adhesion over extended period of time. The animals that are capable of climbing vertical walls and/or surfaces have an ability to sense how well they are adhered to walls and/or surfaces. For example, certain biological species such as the flat-tailed house gecko, Cosymbotus platyurus, senses loss in adhesion in the front feet and uses its tail to counteract the pitch back moment and

regain adhesion[25]; this is essentially a re-engaging mechanism by the animal to re-attach or re-affirm the adhesive force on the contacting surface. In mimicking the gecko-foot adhesive onto micro-robots, the design of the dry adhesive with an embedded adhesive force re-engaging mechanism is an important consideration for endurance and durability.

Currently, there are large number of research efforts as well as excellent review articles in the literature[26-29] on bio-inspired dry-adhesives that describe their fabrication techniques, design and characterization of adhesion strength. The current review article focuses on analysing the state of development of dry adhesive for applications such as micro-robots emphasizing the design considerations to achieve durability. As necessary, we will refer readers to the details presented in existing review articles to avoid redundancy.

Adhesives for micro-climbing robot applications must meet the following requirements: (1) adhesive strength requirements for climbing micro-robots, (a) fiber structural design: multiscale/ hierarchical structures,(b) effect of terminal tip geometry, (c) interplay between intrinsic properties of materials and structural designs, (2) durability, (a) angled fibrillar structures, (b) effect of anisotropic shape on durability, and (3) endurance. The discussion in this review article is organized into the above-mentioned requirements.

2. Adhesive strength requirements for climbing micro-robots

Intuitively, the required adhesion strength scales with the mass of the micro-robots. In nature, insects exhibit an increase in adhesive strength through a higher fibril density to support their weight. Figure 2 shows a correlation between hair/fibril density and the body mass. Typical body mass of animals climbing with adhesive pads varies over seven orders of magnitude from the smallest arthropods (example: mites) to the largest geckos. Nevertheless, area available for

adhesive pads scales with an animal's surface area, which grows slowly compared to body mass. Therefore, design of biological adhesive pads has been adjusted to contain more hair/fibril density to sustain a larger force per area with increase in the mass from arthropods to geckos. An increase in the fibril density is associated with an increase in adhesion with a gecko foot exhibiting the highest adhesive force. As an example, the Tokay gecko footpad consists of approximately 14,400 setae per mm^2 and each seta produces an adhesive force of 6.3 μN. Two front feet of a Tokay gecko collectively produces an adhesive force of 20 N over a surface of 227 mm^2 [17, 30]. A review article detailing the adhesive mechanism of gecko foot pad is published by Autumn *et al.*[31].

Table 1 shows a variety of micro-robots with mass ranging from about 70 - 370 g, and the reported dry adhesive force from 60-3000 mN. From these prior studies, there is no direct correlation between the mass or size of the micro-robots with the optimum adhesive strength used. A design rule is yet to be derived relating the adhesive force requirement of micro-robot to the mass, size, or any other parameters that determine the applicability of dry adhesive for real-life application. We recognize that the method of adhesion strength measurement is also important in order to perform fair comparisons across different fabrication techniques. However, this issue cannot be addressed without complete information on the detailed test methods and effective sample size. Table 1 shows the compiled data containing relevant parameters (not exhaustive) used for designing of the adhesive pads for micro-robots. These parameters include mass, size of robot, its climbing speed, adhesive material, adhesive structure and the optimum adhesive strength. This compiled data serves as a knowledge base and will be useful for researchers working on fabrication and design of adhesives for micro-robots.

Table 1 A summary from literature survey on climbing robots using flat or structured dry polymer adhesives.

Robot's Name	Robot's Size (cm x cm)	Robot's Weight (g)	Dry Adhesive Material	Dry Adhesive Structure	Adhesive Strength (mN)	Climbing Speed (mm/s)	Reference
Stickybot	60 x 20 x 6	370	Polyurethane	Directional fibrillar footpads	NA	40	1
Mini-Whegs	NA	130	Poly(vinyl siloxane)	Structured (pillars with 100 µm high and 40 µm in diameter)	~1200	58	32
Waalbot II	13 x 12.3 x 5	69	Polyurethane	Mushroom shaped	1000	60	33
Tankbot	23 x 14	115	Polyurethane	Flat surface (conveyor thread)	3000	120	34, 35
NA	9 x 11	78	Polyurethane	Angled spatula tip fibers	~ 65	NA	36
NA	NA	240	PDMS	Wedge shaped	~ 500	NA	37
NA	5.4 x 8.9	87	Poly(vinyl siloxane)	Hexagonal pattern (40 µm size)	NA	58	38

2.1 Fiber structural design: multiscale/ hierarchical structures

Adhesives for climbing robots face a challenging requirement in terms of the unpredictable or wide ranging terrains that the robots are expected to walk/climb on. Most surfaces are macroscopically rough with micro or nano scale asperities. Surfaces such as painted walls, carpet, glass windows, wooden floors, and concrete floors contain various degrees of roughness. The hierarchical structure in a gecko-foot pad provides the animal an ability to conform to various roughness asperities and achieve intimate contact with the opposing surfaces. Rodriguez and colleagues in their study show that optimum adhesion is achieved when the dimension of the synthetic fibrillar structures matches with that of the roughness scale of the contacting surface [39]. The adhesive structure which is most relevant to the natural structures was recently analysed in a study by Cañas *et al.*[40]. Their study demonstrated that micro-patterned

surfaces do not adhere to surfaces when the scale of the roughness is much smaller than and much larger than the fiber size[40]. In another report, high aspect ratio structure with nanoscale branches at the tip is shown to demonstrate 150% improvement in adhesion strength when compared to a similar structure with tip branching [41]. These findings suggest that synthetic adhesives with hierarchical architecture can adapt to a wide range of roughness scales and hence can adhere to various surfaces similar to their biological counterparts.

It is known that van der Waals (vdW) forces between a fibril and a surface scales as A/d^3, where A is the Hamaker constant, and d is the separation distance between an individual fibril and the surface[31]. This relationship suggests that separation distance between the fibrils and surface has great influence on the vdW forces. Thus for climbing applications, it is necessary that the synthetic dry-adhesives make intimate contact with surface. Studies demonstrate that natural systems have evolved to achieve superior attachment ability through elaborate hierarchical hairy structures consisting of fine sized contact fibrils (spatulae)[17, 22, 31, 42]. In natural systems, each single setae is subdivided into multiple smaller contacts (spatulae). This fibrillar design provides multiple levels of compliance. For example, the hierarchical design provides conformability to individual setae at the ~ 50 μm scales, and the contact splitting provides conformability to an individual spatulae at the ~ 500 nm scales[42]. These scale effects imply that the setae provide the first level of hierarchy allowing structural adaptability, and the second level of hierarchy obtained using spatulae ensures that the structure is able to adapt to local surface irregularities. Thus, the splitting of a single contact (setae here) into hundreds of multiple smaller contacts (spatulae here) permits the adhesion to wide range of surfaces including smooth surfaces.

Fibrillar design reduces the effective elastic modulus of the structure and ensures that the structure is complaint and able to conform to surfaces. According to the design of the structures

in natural systems, fibrillar design with two or more levels of hierarchy is necessary to optimize the adhesion in synthetic structures. Some of the early studies enhanced adhesion of single-level polymer pillar design fibrils by splitting the single fibril into multiple smaller contacts. For example, Chung *et al.*[43] demonstrated that contact splitting can be highly advantageous for enhancing the adhesion. Similarly, Northen *et al.*[44, 45] fabricated multiscale structures by growing nano sized polymer rods on top of micron sized high aspect ratio pillars. The effect of aspect ratio on resultant adhesive strength is depicted in Figure 3. An enhanced adhesion is reported with the help of this multilevel conformable system. The splitting of single polymer fiber into multiple smaller fibrils also mimics the 'hairy' structure of natural materials.

2.2 Effect of terminal tip geometry

It is well known that the adhesion between the natural fibrillar structures and contact surface is free of hydrogen bonding and arises essentially from intermolecular forces such as van der Waals (vdW) forces[16, 17, 31, 46]. This finding suggests that the adhesion is not chemistry dominated, but in fact depends on the size and geometry of the structures. Gao and Yao[47] used fracture mechanics concepts to demonstrate that robust adhesion can be achieved when the size of the fibers is below a critical size ($r_c = 8E^*\Delta\gamma/\pi\sigma^2$). Where, E^* is the effective modulus of the fiber with respect to the substrate, $\Delta\gamma$ is the work of adhesion, whereas σ is the uniform pressure applied over the contact region of the two contacting bodies. According to fracture mechanics concepts, when two elastic bodies are adhered to one another by vdW forces and when external pull-off force is applied to separate the bodies, stress concentrations are induced at the region near the joint edges. Once the stress concentrations in these regions reach a critical level, "fracture" occurs at the interface between the bodies, and a "crack" begins to propagate. In such cases, failure occurs due to crack propagation. However, Gao *et al.* report that when the size

of the fiber is reduced below a critical size, the material becomes insensitive to flaws or asperities, and the structure attains its theoretical adhesive strength[47].

Adhesives based on extremely small contact elements such as CNTs with diameters between 10 - 50 nm have little or no influence of tip-contact shape on the adhesion properties. However, for adhesives obtained using polymer fibrils of diameter greater than 1 μm, the shape of the fibril's tip-contact has a great influence on its adhesion[48]. Optimal tip geometry for polymer fibrils that have dimensions greater than ~ 1 μm is essential to uniformly distribute the stress. It is estimated that polymer fibers with optimal tip shape can display a theoretical pull-off force which is ~ 50 - 100 times higher than polymer fibrils with poor tip geometry[48]. This result is well supported by recent experimental studies that illustrate the strong influence of tip shape on the adhesion behaviour of the fibrils[49, 50]. Figure 4 shows some examples of tip shapes used in fabrication of synthetic dry-adhesives.

Spolenak *et al.*[51] observed that the effect of different contact shapes on adhesion is prominent for larger contact sizes and stiffer materials. Although flat contact provides maximum adhesion for perfectly smooth surfaces, such contact is found to be very sensitive to surface roughness and dirt. The adhesion of synthetic fibrils with mushroom shaped tips is found to be 3 - 30 times greater than the fibrils with flat end tips or sphere shaped tips. It is attributed to the mushroom shaped tip design which is efficient in removing the stress concentration that is commonly encountered in case of fibrils with simple pillar geometry. Detachment of the fibrils with mushroom shaped tips is essentially controlled by cavitation which is in contrast to the detachment mechanisms of pillar shaped fibrils. For example, del Campo *et al.*[50] fabricated asymmetric elastomeric fibrils by pressing the precursor fibrils against a flat substrate and then curing the fibrils. The elastomeric fibrils with flat ends similar to the natural spatulae design had

30 times greater adhesion compared to the fibrils with spherical or flat tips. Similarly, Davies *et al.*[52] fabricated micron sized polyimide and PDMS fibrils with spatulae like tips and reported that they had better adhesion properties compared to their counterparts with flat tips. These results are attributed to the increased tip contact area at the mushroom shaped tips-surface interface.

Kim *et al.*[53] report that polyurethane fibers with flat spatulae-like tips demonstrate adhesion of 18 N/cm^2 for a preload pressure of 12 N/cm^2. They report that work of adhesion per elastomeric fibers with larger diameter tip increases as the fibrils are capable of elongating and dissipating energy. Additionally, the effective elastic modulus of the structure is not influenced by the tip shape. They explain that low effective elastic modulus and increased contact area increases the adhesion of fibrils with mushroom shaped tips.

2.3 Interplay between intrinsic properties of materials and structural designs

Recent studies demonstrate that the fine size of the contact elements (spatulas), shape, density, aspect ratio as well as the hierarchical design play an important role for their function as attachment structures[46, 49, 50, 54]. Hence, to duplicate the gecko's climbing ability, an in-depth understanding of the relationship of the materials' modulus, size and geometry on adhesion is utmost important.

In natural systems, the setae are composed of stiff β-keratin with an elastic modulus of ~ 2 GPa, which is four orders of magnitude higher than the upper limit of Dahlquist's criterion for tack[18]. Despite its high stiffness, an individual setae is capable of generating ~ 200 μN adhesion force in shear and ~ 40 μN in normal directions against smooth glass substrate[16, 17]. Each foot of a gecko consisting of roughly half a million setae is capable of generating an adhesive force of ~ 100 N, which equals ten times the body weight of the animal[19]. How does the structure composed of stiff β-keratin fibrils function as an attachment device? The arrangement of the

setae fibrils in an array design lowers the effective modulus of the structure and permits it to behave as soft material similar to conventional pressure-sensitive adhesives[18]. The splitting of single setae into hundreds of smaller spatulae and high aspect ratio of the setae shafts reduces the effective elastic modulus of the structure to be less than 100 kPa, which satisfies the Dahlquist's criterion for tack[18]. This splitting effect permits them to act as flexible attachment structures. The fibrillar design of the structure allows increased compliance between the fibers and the target surface, ensuring that they easily conform to the irregularities of the surfaces.

This biological adhesive system has inspired researchers to fabricate synthetic fibrillar structures that can mimic the conformability of natural systems and secure strong adhesive bond with wide variety of surfaces[33, 42]. These findings suggest that synthetic fibrils should possess elastic modulus and yield strength that closely mimic the tensile properties of individual keratinous setae. Carbon nanotubes (CNTs), stiff polymers (~ 1 - 3 GPa stiffness) and elastomers are major types of materials that have been investigated as candidates for the fabrication of dry-adhesive analogue materials[19-23]. Table 2 shows a summary of modulus of materials, structures and adhesive forces. Figures 5A and 5B depict the correlation between the young's modulus and adhesive strength for high aspect ratio and hierarchical adhesive structure, respectively.

Table 2 Summary of synthetic dry adhesives based on modulus of materials and structures.

Material	Fabrication Process	Dimensions (d, L)	Structure	Preload (N/cm^2)	Normal Pull-Off Adhesion (N)	Shear Adhesion (N)	Reference
Polyurethane (E ~ 300kPa)	Three parts molding	380 µm, 1000 µm	Directional stalk	0.25	1	1	48
Polyurethane (E ~ 3 MPa)	Molding	35 µm, 100 µm	Angled microfiber	NI	5	10	21, 55
Polyvinylsilo-xane (E ~ 3 MPa)	Molding	(d_b = 60, d_m = 35, d_t = 25 µm)*, 100 µm	Mushroom shaped	2	0.4	-	56
Polyurethane acrylate (E ~ 19.8 - 320 MPa)	Replica molding and post e-beam irradiation	(d_b = 100, d_t = 80 nm),1 µm,	High aspect ratio (10)	0.3	0	11	57
Polyurethane acrylate (E ~ 19.8 - 320 MPa)	Replica molding and post UV radiation curing	(d_b = 700, d_t = 350 nm),~2.8 µm	Slanted nano hairs	0.3	NI	78	22
Polypropylene (E ~ 1.5 GPa)	Molding	0.6 µm, ~18 µm	Angled microfibers	0.1	0	9	58
PDMS (E ~ 1.8 MPa)	Replica molding and post UV treatment	10 µm, 20 µm	Wedge shaped	0.25	0.5	1.7	33, 59
Beta keratin (E ~ 1-3 GPa)	Nature	(0.2 - 0.5 µm), 3 -130 µm	Gecko foot hair	0.01	1	10	16

Polyimide (E ~ 2 GPa)	Photolitho-graphy	7 µm, 24 µm	Mushroom shaped	-	0.52	-	52
PMMA (E ~ 1.8 - 3.1 GPa)	Molding with post UV exposure	~ 80 nm, ~1.5 - 2 µm	High aspect ratio (>20)	<1	0	3	60
Polyimide (E ~ 3 GPa)	Molding followed by oxygen plasma etching	0.2 - 4 µm, 0.15 - 2 µm	High aspect ratio	50	3	NI	61
MWCNTs (bundled) (E ~ 1000 GPa)	Chemical vapor deposition	20 - 30 nm, 5- 100 µm	High aspect ratio	500	0.5	0.6	62
MWCNTs (bundled) (E ~ 1000 GPa)	Chemical vapor deposition	8 nm, ~200–500 µm	High aspect ratio	50	0.8	6	20
SWCNTs (bundled) (E ~ 1000 GPa)	PECVD	~2 nm, ~5 - 19 µm	High aspect ratio	125	5	2.5	63
MWCNTs (bundled) (E ~ 1000 GPa)	Low-pressure CVD	10 - 15 nm, ~150 µm	High aspect ratio	125	3	16	64
MWCNTs (bundled) (E ~ 1000 GPa)	Chemical vapor deposition	~ 5 nm, 700 -1000 µm	High aspect ratio	50	-	45	65

* Here, d_b stands for base diameter, d_m stands for middle diameter and d_t stands for top diameter of the major structure fabricated.

3. Durability

One notable feature of biological adhesives is that they can be used repeatedly without losing their adhesive performance, which allows the animal to climb surfaces for an extended period of time. In contrast to biological structures, the adhesive performance of synthetic adhesives is often seen to degrade after just a few attachment-detachment cycles. The adhesive performance of synthetic structures reduces due to contamination, buckling of polymer fibrils, bunching of fibrils, plastic deformation of the polymer during the pull-off, and excessive pre-loads.

Durability of an adhesive structure can be determined by evaluating its adhesive performance after repeated use and comparing it with its adhesive performance after the first attachment-detachment cycle. Gorb *et al*.[66] demonstrated the degradation of adhesive performance after 100 attachment-detachment cycles using mushroom shaped adhesive.

Another approach is to examine for contamination or wear of the structures after each attachment-detachment cycle using scanning electron microscope (SEM). SEM images are also taken on the target surface to determine if any residue is left over, which would suggest that the fibrils from the structures are damaged. The latter approach is challenging as it involves tedious analysis and difficulty to obtain reliable data.

The adhesive structures of biological systems have been shown in the laboratory to be reusable for over 30,000 cycles[54]. Their durability is attributed to its hierarchical design that distributes the load evenly among all setae-spatulae fibrils. This desired property of durability needs to be incorporated while designing adhesive pads for climbing robots, allowing them to maintain their adhesive performance over numerous attachment-detachment cycles.

3.1 Angled fibrillar structures

Few studies such as by Santos *et al.*[48] and Gorb *et al.*[56] have successfully demonstrated the reusability for over ~ 100 attachment-detachment cycles when the adhesive structures are composed of angled stalks or when the terminal end on the fibrils are mushroom shaped (see Figure 6). Lee *et al*. fabricated adhesive structures using stiff polypropylene fibers with potential applications for climbing robot[58]. The structures demonstrated peel strength of 0.15 N/m, which ensures that the structure can easily detach during vertical climbing. They show that the shear force of the structure increases with distance, implying resistance to slip during climbing. Additionally, the shear adhesion of the structures increased with number of tests when tested for 50 times. They attribute this finding to the angling of the fibers in the shear direction that helped reduce the height variation within the structure. This finding suggests that angled structures maybe appropriate for reusable and durable adhesive intended for climbing.

Parness *et al*.[54] demonstrated that tapered beam (wedge-shaped structures) structures maintained ~ 67% of its initial adhesion even after ~ 30,000 cycles. It is suggested that the high value of pull-off force to preload ratio makes the structure reusable as it prevents damage to the fibrils during loading. Thus, for the adhesive to be durable, damage to the fibrils should be minimized. Complaint material that is able to bend and deform elastically instead of fracturing is essential to ensure minimum damage to the fibrils. Similar to natural systems, a multilevel hierarchical design should be used, which would ensure equal load sharing and generate increased level of adhesion. The summary of recent studies on durability of the adhesives is shown in Table 3.

Table 3 Summary of exemplar polymers with their adhesive force and durability.

Material	Structure	Dimensions (d, L)	Preload (N/cm^2)	Test Area (cm^2)	Substrate Tested On	Adhesive Force (N)	Durability (cycles)	Reference
Polyurethane (E ~ 300 kPa)	Directional stalk	380 µm, 1000 µm	0.25	3.9	Glass	1.0	>100	48
Polyvinylsiloxane (E ~ 3 MPa)	Mushroom shaped	(d_b = 60, d_m = 35, d_t = 25 µm), 100 µm	2	0.066	Glass	0.4	>100	56
Polypropylene (E ~ 1 GPa)	Microfibre arrays	0.6 µm, 18 µm	< 0.1	0.01	Spherical indenter	0.003	150	1, 67, 68
Gecko setae array (E ~ 1-3 GPa)	Hierarchical	(0.2 - 0.5 µm), 3 -130 µm	35 µm preload depth ($LDPa_{vg}$ protocol)	0.0093	Glass	0.45	>30000	16, 69
PDMS (E ~ 1.8 MPa)	Wedge shaped	10 µm, 20 µm	< 0.06	1	Sapphire hemisphere lens	0.51	>30000	33, 59

3.2 Effect of anisotropic shape on durability

Structures that require low forces to attach as well as detach and that have a high pull-off force to preload ratio are highly useful for climbing applications. Climbing is an energy intensive process, and low attachment forces as well as detachment forces ensure that the energy expenditure while climbing is minimized. For example, structures that easily attach to surfaces require low preload in the normal direction that tends to push the artefact, such as a robot, off the climbing surface[1]. Similarly, structures that peel off easily at certain angles will reduce the force required to detach the structure. Autumn *et al.*[16, 31] as well as Kim *et al.*[1] demonstrate that the adhesive structures of natural materials are directional, i.e., depend on the relative direction of applied load, based on performing adhesion measurements on single setae. They found that when the setae is preloaded in both perpendicular and parallel directions, the pull off force is 10 times higher than when the setae is preloaded in the perpendicular direction only. By applying a perpendicular preload combined with a parallel drag preload, they demonstrate that the adhesive force of individual setae average 194 μN. These results show setae attachment to have strong directionality. Additionally, the detachment of setae occurred at an angle ~30° between the setal stalk and substrate. They also show that at a critical angle of ~30° the detachment of the setae is independent of the adhesive force. They argue that setal contact must be within 30° of the surface for biological systems.

This feature when combined with the hierarchical fibrillar design allows the structures to adhere to surfaces by using small pre-load force. Recent studies have incorporated this design for fabrication of synthetic dry-adhesive[21, 58]. Such structures with slanted fibrils adhere to surfaces only when loaded in a particular direction. Further, they demonstrate that low attachment/detachment forces and high pull-off force to preload ratio can be obtained

using adhesive structures that are slanted an angle. Additionally, theory suggests that the effective modulus of the structure can be lowered with the help of angled structures. The effective elastic modulus (E_{eff}) of slanted structures is given by

$$E_{eff} = \frac{3EID \sin\theta}{L^2 \cos^2\theta[1 \pm \mu \tan\theta]} \quad (1)$$

where E is the modulus of the fibril, I the moment of inertia, D density of the fibrils, L the length of the fibrils, θ is the slanted angle and μ is the coefficient of friction.

Equation 1 shows that, apart from the structure hierarchy, fine size of the fibril and fibril density, the slanted angle of the structures is crucial for reducing the effective modulus of the structures. Aksak and Murphy *et al.*[21] fabricated directional adhesives using polyurethane and demonstrated that these adhesives have strong adhesive force of ~ 10 N/cm^2 in the gripping direction whereas the structures show weak adhesion of ~ 2 N/cm^2 in the detachment direction. Similar structures were fabricated by Kim *et al.*[1] using an e-beam exposure method. The fabricated angled nano-hairs demonstrated directional shear adhesion. The adhesion force in the forward direction was reported to be ~11 N/cm^2, whereas the adhesion in the reverse direction was 2.2 N/cm^2. In yet another study, Jeong *et al.*[22] fabricated hierarchical patterned polymer 'hairy' structures to obtain directionally sensitive adhesives. By controlling the leaning angle, size, tip shape and hierarchical structures, the structures exhibited strong shear forces of ~ 26 N/cm^2 in the angled direction. In the opposite direction, the structure was able to easily detach with a force of ~ 2.2 N/cm^2.

The high adhesive performance of these polymer structures were attributed to the reduced elastic modulus of ~ 26.3 kPa, and the geometry including the hierarchical design, directional angle and shape of the contact.

4. Endurance

One unique feature of a gecko is its ability to support its own weight while hanging from ceilings, and remain attached for extended periods of time. Mimicking this feature of natural materials can open up opportunities to design next generation of dry-adhesives that can be used for applications such as climbing robot, and, more specifically for surveillance robot applications that require the adhesive to hold the mass of a stationary robot for long periods of time. Here, we refer to endurance as this ability of adhesives to maintain adhesion for extended periods of time. While considerable progress has been made in improving the adhesion of dry-adhesives and investigating their use for robot applications[1, 36, 37, 48, 55, 56, 70-72], not many articles currently exist in the literature that demonstrate and characterize the endurance of synthetic adhesives.

As opposed to pressure-sensitive adhesives fabricated using soft viscoelastic materials that quickly wear out over time, the adhesion of natural dry-adhesive setae-spatula structures can last for months under 'real-world conditions'[18, 73]. Further, they are capable of maintaining adhesion for extended period of time as they have the ability to resist local deformation and/or structural failure. In the case of pressure-sensitive materials, the viscoelastic materials used to achieve adhesion exhibit plastic deformation which leads to an increase the area of contact with the substrate's surface at the molecular scale. When these pressure-sensitive adhesives are being detached from the surface, elongation of the polymer chains leads to the formation of bridge-like structures called crazes between the adhesive material and the surface. In this case, the total fracture energy is increased as it not only includes the work that must be done on the craze, but also includes the work required to break the adhesive bonds at the interface[30]. This phenomenon ensures that pressure-sensitive adhesive can achieve high adhesion when they come in contact with a surface. However, since soft polymers are used in pressure-sensitive adhesives, the material is prone to creep,

fouling and self-adhesion. These attributes of pressure-sensitive adhesives pose problems for their durability and ability to adhere for extended periods of time.

On the other hand, 'hairy' fibrillar designs used to fabricate dry-adhesives ensure that the effective modulus of the structures satisfy the Dahlquist's criterion for tacky materials. Hence, the structure acts like a soft, sticky and deformable material. Despite this characteristic, individual fibrils have good mechanical integrity as they are composed of stiff keratin proteins, which ensure that the material does not experience creep. These features make the adhesive not only durable, but also enable it to adhere to surfaces with a constant load for an extended period of time. Jagota *et al.*[30] in their study demonstrate that because of the fibrillar design, the structure requires higher fracture energy to detach from the surface compared to a bulk solid layer of adhesive. Fibrils in dry-adhesives act in a manner similar to crazes in pressure-sensitive adhesives. Here, in fibrillar structures, each fibril stores elastic energy which is released and dissipated internally when an individual fibril is detached from the substrate. The mechanism of energy dissipation in fibrillar structures differs with that of crazes in pressure-sensitive adhesives that dissipate energy plastically. This mechanism indicates that dry-adhesive analogues that possess two or more levels of hierarchy would require higher energy to detach from surfaces as the elastic energy dissipated when each fibril is pulled apart does not contribute to propagate the crack. Furthermore, stiffness of the material used for the fabrication of dry-adhesives can also play a role in an adhesive's endurance. A softer material can make the structure tackier, but the material can also undergo plastic deformation and creep. On the other hand, a stiffer material can increase the overall effective modulus of the structure such that it no longer satisfies the Dahlquist's criterion for tacky materials.

Setae-level adhesive forces have been successfully produced at the nano-level using polymer pillars or CNT fibrillar structure [19, 20]. Ge *et al.*[20] developed synthetic adhesive tape

based on CNT arrays and demonstrated that the structure can support shear strength of 36 N/cm^2, which is nearly four times higher than natural systems. These CNTs are arranged and bundled such that predetermined square patches with widths ranging from 50 to 500 μm are obtained. Such structures can support four to seven times higher shear force compared to unpatterned structures. Furthermore, the ability of these structures to maintain stable shear adhesive force is investigated and compared with that of pressure-sensitive viscoelastic tape. The results show that the synthetic adhesive tapes are stable and capable of maintaining the shear stress of ~20 N/cm^2 for 8-12 h duration (see Figure 7). On the contrary, although pressure-sensitive adhesive tapes have stronger adhesion compared to synthetic adhesive tape for short duration of time, their ability to maintain shear load decreased with time. This result is typical of viscoelastic materials that tend to creep. The patterned CNT structures supported large shear forces, and when a critical load is reached, a catastrophic rupture is initiated. The results indicate that there is large energy dissipation and the failure is initiated due to cohesive failure mechanisms. The patterning of CNTs hinders the crack growth and play a role to deviate the crack. Thus, the crack needs to be reinitiated at each square pattern before the entire structure can be detached. This effect increases the interfacial adhesive strength and ensures that the structure can support large shear stresses. Ge *et al.* explain that these square patches can be thought to be analogous to the micrometer sized setae, and the individual CNT within each pattern represent the nanometer-size spatula.

In a similar study, Qu *et al.* [64] fabricated CNT arrays with entangled segments on the top of each vertically aligned CNT as shown in Figure 8. These structures are analogous to the natural setae-spatulae structures where the trunk of the CNT mimics the setae while the curly entangled top mimics the spatula. They demonstrate that these structures can support a macroscopic adhesive force of ~ 100 N/cm^2, which is ~10 times higher than that of the natural structures. The endurance of the vertically aligned multiwalled nanotube (VA-

MWNT) structures are also investigated and compared with the commercial copper adhesive tapes. These structures are capable of sustaining shear loading of 40 N/cm^2 or a normal pull away force of 12 N/cm^2 for a period of ~24 h. The structures remained adhered to glass substrates with no cohesive breakage, which demonstrates that the adhesion in these structures is time-independent. On the other hand, the commercial copper adhesive tapes show time dependency. The commercial adhesive tapes under same loads are seen to fatigue easily and detached from the substrate within 1h. The superior durability of the CNT structures is attributed to the entangled segments on top of the CNT that untangles and brings the sidewalls in contact with the surface. The CNTs are then aligned along the loading direction and elastically stretched, which is in contrast to plastic deformation in case of viscoelastic materials.

Polymer based structures have become a popular choice as they are relatively easier to fabricate and their geometry can be easily controlled using various fabrication techniques. The superior processibility and scalability of polymer based dry-adhesive structures makes them ideal candidates for climbing robot applications[19]. Recent progress in fabrication techniques have ensured that novel multiscale hierarchical structures similar to the natural material can be obtained using wide variety of polymeric materials[21, 22]. Some studies demonstrate the fabrication of advanced three dimensional structures such as angled array using polymer materials[1, 21, 58]. Such structures display anisotropic properties of dry adhesion. This directional attachment is crucial for climbing robot applications as they generate adhesion when loaded in one direction and detach when the loading is reversed, ensuring that less energy is utilized during the attachment-detachment cycles.

5. Future of gecko inspired dry adhesives

The recent studies of gecko-inspired adhesives show that a hierarchical structure (for instance, see Figure 9) mimicking the natural gecko system is able to obtain intimate contact with surface irregularities and enhance the adhesion performance based on the concept of contact splitting. A variety of surface-structure designs have been fabricated on a variety of materials and a range of dry adhesive strengths has been obtained. A variety of fabrication techniques such as photolithography, plasma etching, deep reactive ion etching, electron beam lithography chemical vapour deposition as well as micro/nano-moulding are being employed to obtain desired adhesive structures that closely mimic the geometry and adhesive mechanisms of natural materials. As discussed earlier, key parameters such as length, diameter, and angle of the hierarchical structures as well as its resultant stiffness are being optimized to improve the adhesive behaviour of synthetic structures. Nevertheless, fabrication process needs to be identified to affordably mass-produce the desired adhesive structure. Photolithography is being considered as one of the possible fabrication processes due to its scalability and affordability to fabricate patterned micro/nano-structures.

Despite the extensive research on gecko-foot mimetic dry adhesive, a major challenge remains in the practicality of gecko-foot mimetic dry adhesive, especially in terms of reusability or durability. Durability and reusabiltiy of gecko-mimetic structures have not been fully investigated partly due to the different techniques used to quantify durability. In addition, the intrinsic property of the material used for making gecko-foot mimetic structures plays an important role in determining the durability of the dry adhesive; although a variety of polymeric materials and synthetic nanomaterials have been investigated. These materials include polymers such as polyimide, polyurethane, polypropylene, and polydimethylsiloxane as well as synthetic nanomaterials such as carbon nanotubes. Despite this, there is still plenty of room for material innovations in order to balance the ease of fabrication and the mechanical properties. By balancing surface structural design with a material with good

mechanical stability, practical and durable dry adhesive may result. (Durability as explained in earlier section refers to repeated attachment and detachment.)

The potential of using bio-inspired adhesives are not only applicable for applications such as climbing robots, but for many domestic applications such as wall mounted devices, fixing household items, medical application as bandage, fastening agent for temporary construction.

6 Acknowledgements

This study is based on STARS (Systems Technology for Autonomous Reconnaissance and Surveillance) project funded by Temasek Laboratories @SUTD. The authors will also like to acknowledge the support of SUTD-MIT International Design Centre (Project No: IDG31400101).

7 References

1. S. Kim, M. Spenko, S. Trujillo, B. Heyneman, D. Santos and M. R. Cutkosky, *IEEE Trans. Robot.*, 2008, **24**, 65-74.

2. M. J. Spenko, G. C. Haynes, J. A. Saunders, M. R. Cutkosky, A. A. Rizzi, R. J. Full and D. E. Koditschek, *J. Field Robot.*, 2008, **25**, 223-242.

3. A. T. Baisch, P. Sreetharan and R. J. Wood, 2010 IEEE/RSJ International Conference on Intelligent Robots and Systems (IROS), Taipei, 2010.

4. W. Brockmann, in *Climbing and Walking Robots*, Springer, 2006, pp. 107-114.

5. K. Berns, T. Braun, C. Hillenbrand and T. Luksch, in *Climbing and Walking Robots*, Springer, 2005, pp. 981-988.

6. V. Singh, S. M. Skiles, J. E. Krager, K. L. Wood, D. Jensen and R. Sierakowski, *J. Mech. Des.*, 2009, **131**, 081010.

7. V. Singh, B. Walther, K. Wood and D. Jensen, in *Tools for Innovation: The Science Behind the Practical Methods That Drive New Ideas*, Oxford University Press, USA, 2009.

8. J. Weaver, K. Wood, R. Crawford and D. Jensen, *J. Comput. Inf. Sci. Eng.*, 2010, **10**, 031012.

9. P. Pace, Wood, K., Wood, J., Carson, J., Jensen, D., and Skibba, B, *ASEE Annual Conference, Vancouver, BC, Canada, Session M449A Outstanding Contributions: Mechanical Engineering Education*, 2011.

10. N. Xuelei, Suherlan, A.P., Soh, G.S., Foong, S., Wood, K.L. and Otto, K.N., *The 13th International Conference on Control, Automation, Robotics, and Vision, ICARCV,* Singapore, 2014.

11. R. Sosa, Rajesh, M., and Wood, K.L., *Proceedings of the ASME 2014 International Design Engineering Conferences & Computers and Information in Engineering Conference, IDETC/CIE 2014, Buffalo, NY,* 2014.

12. H. Homann, *Naturwissenschaften*, 1957, 44, 318-319.

13. U. Hiller, *Z. Morph. Tiere*, 1968, **62**, 307-362.

14. E. Bauchhenss, *Zoomorphologie* 1979, 93.

15. N. Stork, *J. Exp. Biol.*, 1980, **88**, 91-108.

16. K. Autumn, Y. A. Liang, S. T. Hsieh, W. Zesch, W. P. Chan, T. W. Kenny, R. Fearing and R. J. Full, *Nature*, 2000, **405**, 681-685.

17. K. Autumn, M. Sitti, Y. A. Liang, A. M. Peattie, W. R. Hansen, S. Sponberg, T. W. Kenny, R. Fearing, J. N. Israelachvili and R. J. Full, *Proc. Natl. Acad. Sci. U. S. A.*, 2002, **99**, 12252-12256.

18. K. Autumn, C. Majidi, R. Groff, A. Dittmore and R. Fearing, *J. Exp. Biol.*, 2006, **209**, 3558-3568.

19. S. Hu, Z. Xia and L. Dai, *Nanoscale*, 2013, **5**, 475-486.

20. L. Ge, S. Sethi, L. Ci, P. M. Ajayan and A. Dhinojwala, *Proc. Natl. Acad. Sci. U. S. A.*, 2007, **104**, 10792-10795.

21. B. Aksak, M. P. Murphy and M. Sitti, *Langmuir*, 2007, **23**, 3322-3332.

22. H. E. Jeong, J.-K. Lee, H. N. Kim, S. H. Moon and K. Y. Suh, *Proc. Natl. Acad. Sci. U. S. A.*, 2009, **106**, 5639-5644.

23. A. Mahdavi, L. Ferreira, C. Sundback, J. W. Nichol, E. P. Chan, D. J. D. Carter, C. J. Bettinger, S. Patanavanich, L. Chignozha, E. Ben-Joseph, A. Galakatos, H. Pryor, I. Pomerantseva, P. T. Masiakos, W. Faquin, A. Zumbuehl, S. Hong, J. Borenstein, J. Vacanti, R. Langer and J. M. Karp, *Proc. Natl. Acad. Sci. U. S. A.*, 2008, **105**, 2307-2312.

24. A. M. Peattie, *J. Comp. Physiol. B-Biochem. Syst. Environ. Physiol.*, 2009, **179**, 231-239.

25. A. Jusufi, D. I. Goldman, S. Revzen and R. J. Full, *Proc. Natl. Acad. Sci. U. S. A.*, 2008, **105**, 4215-4219.

26. J. Yu, S. Chary, S. Das, J. Tamelier, N. S. Pesika, K. L. Turner and J. N. Israelachvili, *Adv. Funct. Mater.*, 2011, **21**, 3010-3018.

27. C. Greiner, *Nanotechnologies for the Life Sciences, Wiley-VCH Verlag GmbH & Co. KGaA*, 2012, 1.

28. Y. Menguc and M. Sitti, in *Polymer Adhesion, Friction, and Lubrication*, Wiley, 2013, p. 351.

29. A. Pattantyus-Abraham, J. Krahn and C. Menon, *Front. Bioeng. Biotechnol.*, 2013, ***1***, 22.

30. B. S. Jagota AJ, *Integr. Comp. Biol.*, 2002, **42**,1140-1145.

31. K. Autumn and A. M. Peattie, *Integr. Comp. Biol.*, 2002, **42**, 1081-1090.

32. K. A. Daltorio, T. E. Wei, G. D. Wile, L. Southard, L. R. Palmer, S. N. Gorb, R. E. Ritzmann and R. D. Quinn, IEEE/RSJ International Conference on Intelligent Robots and Systems, San Diego, California, 2007.

33. M. P. Murphy, C. Kute, Y. Mengüç and M. Sitti, *Int. J. Robot. Res.*, 2011, **30**, 118-133.

34. O. Unver and M. Sitti, *Int. J. Robot. Res.*, 2010, 0278364910380759.

35. O. Unver and M. Sitti, IEEE International Conference on Robotics and Automation, Kobe, Japan, 2009.

36. B. Aksak, M. P. Murphy and M. Sitti, IEEE International Conference on Robotics and Automation, Pasadena, California, 2008.

37. A. Asbeck, S. Dastoor, A. Parness, L. Fullerton, N. Esparza, D. Soto, B. Heyneman and M. Cutkosky, IEEE International Conference on Robotics and Automation, Kobe, Japan, 2009.

38. K. A. Daltorio, S. Gorb, A. Peressadko, A. D. Horchler, T. E. Wei, R. E. Ritzmann and R. D. Quinn, *MRS Bull.*, 2007, **32**, 504-508.

39. I. Rodriguez, C. T. Lim, S. Natarajan, A. Y. Y. Ho, E. L. Van, N. Elmouelhi, H. Y. Low, M. Vyakarnam and K. Cooper, *J. Adhes.*, 2013, **89**, 921-936.

40. N. Cañas, M. Kamperman, B. Völker, E. Kroner, R. M. McMeeking and E. Arzt, *Acta Biomater.*, 2012, **8**, 282-288.

41. A. Y. Y. Ho, L. P. Yeo, Y. C. Lam and I. Rodríguez, *ACS Nano*, 2011, **5**, 1897-1906.

42. S. Kim, M. Spenko, S. Trujillo, B. Heyneman, V. Mattoli and M. R. Cutkosky, IEEE International Conference on Robotics and Automation, Roma, Italy, 2007.

43. J. Y. Chung and M. K. Chaudhury, *J. R. Soc. Interface*, 2005, **2**, 55-61.

44. M. T. Northen, C. Greiner, E. Arzt and K. L. Turner, *Adv. Mater.*, 2008, **20**, 3905-3909.

45. M. T. Northen and K. L. Turner, *Nanotechnology*, 2005, **16**, 1159.

46. W. Hansen and K. Autumn, *Proc. Natl. Acad. Sci. U. S. A.*, 2005, **102**, 385-389.

47. H. J. Gao and H. M. Yao, *Proc. Natl. Acad. Sci. U. S. A.*, 2004, **101**, 7851-7856.

48. D. Santos, M. Spenko, A. Parness, S. Kim and M. Cutkosky, *J. Adhes. Sci. Technol.*, 2007, **21**, 1317-1341.

49. C. Greiner, R. Spolenak and E. Arzt, *Acta Biomater.*, 2009, **5**, 597-606.

50. A. del Campo, C. Greiner and E. Arzt, *Langmuir*, 2007, **23**, 10235-10243.

51. R. Spolenak, S. Gorb, H. Gao and E. Arzt, *Proc. R. Soc. A-Math. Phys. Eng. Sci.*, 2005, **461**, 305-319.

52. J. Davies, S. Haq, T. Hawke and J. P. Sargent, *Int. J. Adhes. Adhes.*, 2009, **29**, 380-390.

53. S. Kim and M. Sitti, *Appl. Phys. Lett.*, 2006, 89.

54. A. Parness, D. Soto, N. Esparza, N. Gravish, M. Wilkinson, K. Autumn and M. Cutkosky, *J. R. Soc. Interface*, 2009, **6**, 1223-1232.

55. M. P. Murphy, B. Aksak and M. Sitti, *Small*, 2009, **5**, 170-175.

56. S. Gorb, M. Varenberg, A. Peressadko and J. Tuma, *J. R. Soc. Interface*, 2007, **4**, 271-275.

57. T. I. Kim, H. E. Jeong, K. Y. Suh and H. H. Lee, *Adv. Mater.*, 2009, 21, 2276-2281.

58. J. Lee, R. S. Fearing and K. Komvopoulos, *Appl. Phys. Lett.,* 2008, **93**, 191910.

59. M. P. Murphy and M. Sitti, *IEEE-ASME Trans. Mechatron.*, 2007, **12**, 330-338.

60. H. E. Jeong, S. H. Lee, P. Kim and K. Y. Suh, *Colloid Surf. A-Physicochem. Eng. Asp.*, 2008, **313**, 359-364.

61. A. Geim, S. D. I. Grigorieva, K. Novoselov, A. Zhukov and S. Y. Shapoval, *Nat. Mater.*, 2003, **2**, 461-463.

62. Y. Zhao, T. Tong, L. Delzeit, A. Kashani, M. Meyyappan and A. Majumdar, *J. Vac. Sci. Technol. B*, 2006, **24**, 331-335.

63. L. Qu and L. Dai, *Adv. Mater.,* 2007, **19**, 3844-3849.

64. L. Qu, L. Dai, M. Stone, Z. Xia and Z. L. Wang, *Science*, 2008, **322**, 238-242.

65. Y. Maeno. Y. Nakayama, *Appl. Phys. Lett*, 2009, 94.

66. M. Varenberg and S. Gorb, *J. R. Soc. Interface*, 2007, **4**, 721-725.

67. J. Lee, C. Majidi, B. Schubert and R. S. Fearing, *J. R. Soc. Interface*, 2008, **5**, 835-844.

68. B. Schubert, J. Lee, C. Majidi and R. S. Fearing, *J. R. Soc. Interface*, 2008, **5**, 845-853.

69. N. Gravish, M. Wilkinson and K. Autumn, *J. R. Soc. Interface*, 2008, **5**, 339-348.

70. C. Menon, M. Murphy and M. Sitti, IEEE International Conference on Robotics and Biomimetics, Shenyang, China, 2004.

71. C. Kute, M. P. Murphy, Y. Mengüç and M. Sitti, IEEE International Conference on Robotics and Automation, Anchorage, Alaska, 2010.

72. M. R. Cutkosky and S. Kim, *Philos. Trans. R. Soc. A-Math. Phys. Eng. Sci.*, 2009, **367**, 1799-1813.

73. N. Gravish, M. Wilkinson, S. Sponberg, A. Parness, N. Esparza, D. Soto, T. Yamaguchi, M. Broide, M. Cutkosky and C. Creton, *J. R. Soc. Interface*, 2010, **7**, 259-269.

74. W. Federle, *J. Exp. Biol.*, 2006, **209**, 2611-2621.

75. A. Peressadko and S. N. Gorb, *J. Adhes.*, 2004, **80**, 247-261.

76. C. Greiner, E. Arzt and A. del Campo, *Adv. Mater.*, 2009, **21**, 479-482.

77. A. J. Crosby, M. Hageman and A. Duncan, *Langmuir*, 2005, **21**, 11738-11743.

78. C. Greiner, A. del Campo and E. Arzt, *Langmuir*, 2007, **23**, 3495-3502.

79. B. Chen, P. Goldberg Oppenheimer, T. A. V. Shean, C. T. Wirth, S. Hofmann and J. Robertson, *J. Phys. Chem. C*, 2012, **116**, 20047-20053.

80. B. Yurdumakan, N. R. Raravikar, P. M. Ajayan and A. Dhinojwala, *Chem. Commun.*, 2005, **30**, 3799-3801.

81. M. P. Murphy, S. Kim and M. Sitti, *ACS Appl. Mater. Interfaces*, 2009, **1**, 849-855.

82. H. E. Jeong, R. Kwak, A. Khademhosseini and K. Y. Suh, *Nanoscale*, 2009, **1**, 331-338.

83. J. Lee, B. Bush, R. Maboudian and R. S. Fearing, *Langmuir*, 2009, **25**, 12449-12453.

84. Y. Wang, H. Hu, J. Shao and Y. Ding, *ACS Appl. Mater. Interfaces*, 2014, **6**, 2213-2218.

List of Figures

Figure 1. Figure shows the structural hierarchy of the gecko's 'hairy' adhesive structures (A) Image of a Tokay gecko, (B) image shows the foot of a Tokay gecko, (C) scanning electron microscopy (SEM) image of the foot hair, 'setae' that are found on the feet of the animal, (D) SEM image of a single setae, and (E) image shows that a single setae branches out to multiple stapula (reprinted with permission from ref. 18; Copyright 2006 @ Company of Biologists Ltd).

Figure 2. Plot of density of hair found on the feet of insect and animals as a function of their body mass. It is evident that insects show a linear correlation between hair/fibril density as a function of body Mass (reprinted with permission from ref. 74; Copyright 2006 @ Company of Biologists Ltd).

Figure 3. Plot of normal adhesive strength *versus* aspect ratio. The plot shows a general trend of increase in adhesive strength with aspect ratio of the fabricated structure. The effect of applied preload on the adhesive strength is not considered in this plot as the preload values are not provided by all the studies. The data points in the plot are the adhesive strength values for the following materials: (1) PVS [75], (2) PDMS [76], (3) PDMS [77], (4) PDMS [78], (5) VACNTs [79], (6) PU [55], (7) PVS [56], (8) PDMS [54], (9) PA [52], (10) PA [61], (11) MWCNTs [80], and (12) SWCNTs [63]

Figure 4. SEM images of selected patterns with different tip geometries: (A) flat, (B) spherical, (C) mushroom and (D) spatula. Pillars have a radius of 10 μm and a height of about 20 μm (reprinted with permission from ref. 50; Copyright 2007 @ American Chemical Society).

Figure 5. (A) Normal adhesive strength vs. Young's modulus for high aspect ratio structures: (1) PVS [75], (2) PDMS [76], (3) PDMS [77], (4) PDMS [78], (5) VACNTs [79], (6) PU [55], (7) PVS [56], (8) PDMS [54], (9) PA [52], (10) PA [61], (11) MWCNTs [64], (12) SWCNTs [63], and (13) MWCNTs [80], (B) Normal adhesive strength vs. Young's modulus for two level hierarchical structures: (1) PDMS [76], (2) PU [81], (3) PUA (shear) [22], (4) PC (shear) [41], (5) MWCNTs (shear) [20], (6) Organorods [45], (7) PUA (shear) [82], (8) PDMS (shear) [37], and (9) HDPE (shear) [83]. Data points depict normal adhesive strength unless otherwise specified. The plots show a general trend of increase in adhesive strength with young's modulus of the fabricated structures.

Figure 6. (A) SEM image of biomimetic mushroom-shaped fibrillar adhesive microstructures; and (B) Magnified SEM image of the structure (reprinted with permission from ref. 84; Copyright 2014 @ American Chemical Society).

Figure 7: (A) comparison of shear force supported by natural material, unpatterned CNTs and patterned CNTs, and (B) plot of shear stress supported by synthetic gecko tape and viscoelastic pressure sensitive tape versus time (reprinted with permission from ref. 20; Copyright 2007 @ National Academy of Sciences, U.S.A.).

Figure 8: (A) SEM image of natural aligned elastic setae that branches into spatulas at the tip end, (B) SEM image of CNT with entangled tops resembling the setae-spatula structures, and (C) endurability comparison between avertically aligned multiwalled nanotube (VA- MWNT) and commercial copper adhesive tapes under normal and shear loading. The figure shows that the VA-MWNT structures are capable of maintaining adhesion both in normal and shear loading for ~24 h while the commercial copper tape under the same loading conditions fails within 1h (reprinted with permission from ref. 64; Copyright 2008 @ AAAS).

Figure 9: SEM of three-level hierarchical polyurethane fibers (a) curved base fibers, (b) base fiber tip with midlevel fibers, (c) midlevel fibers in detail, (d) terminal third level fibers at the tip of the midlevel fibers having flat mushroom tips (reprinted with permission from ref. 81; Copyright 2009 @ American Chemical Society).

Figure 1

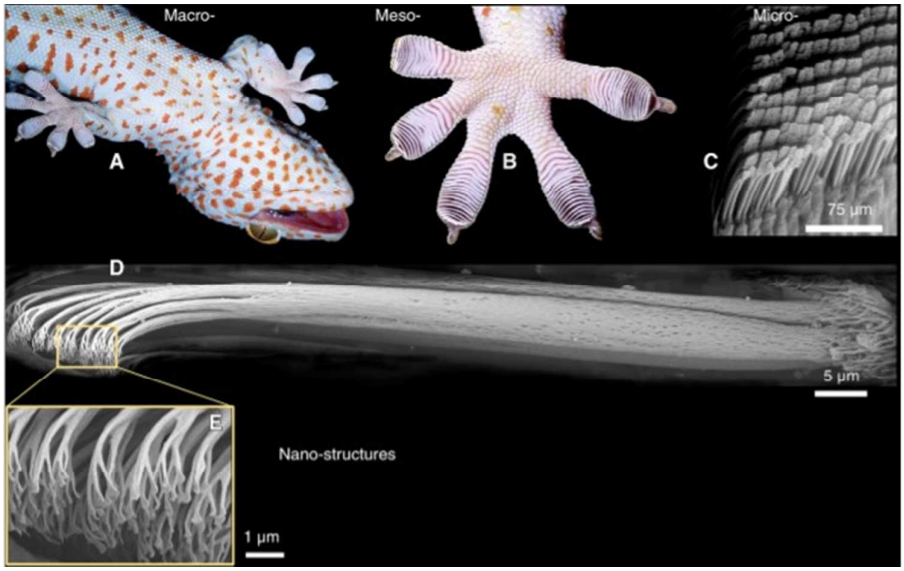

Figure 2

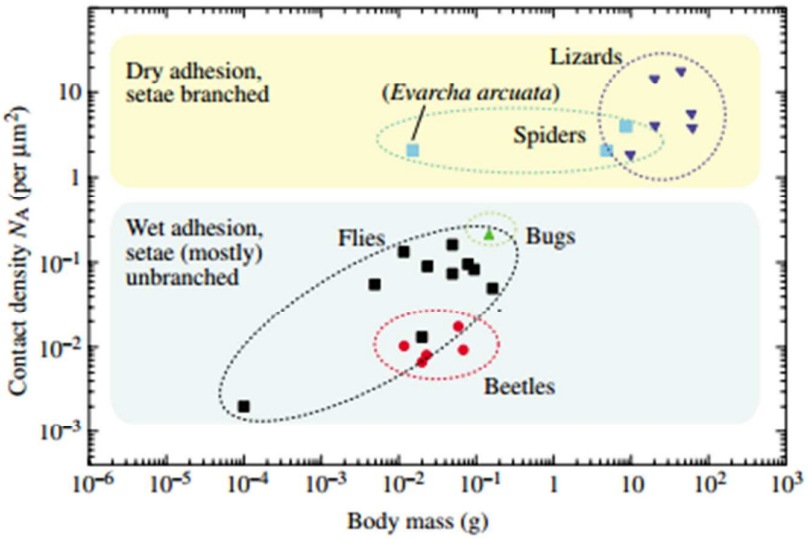

Figure 3

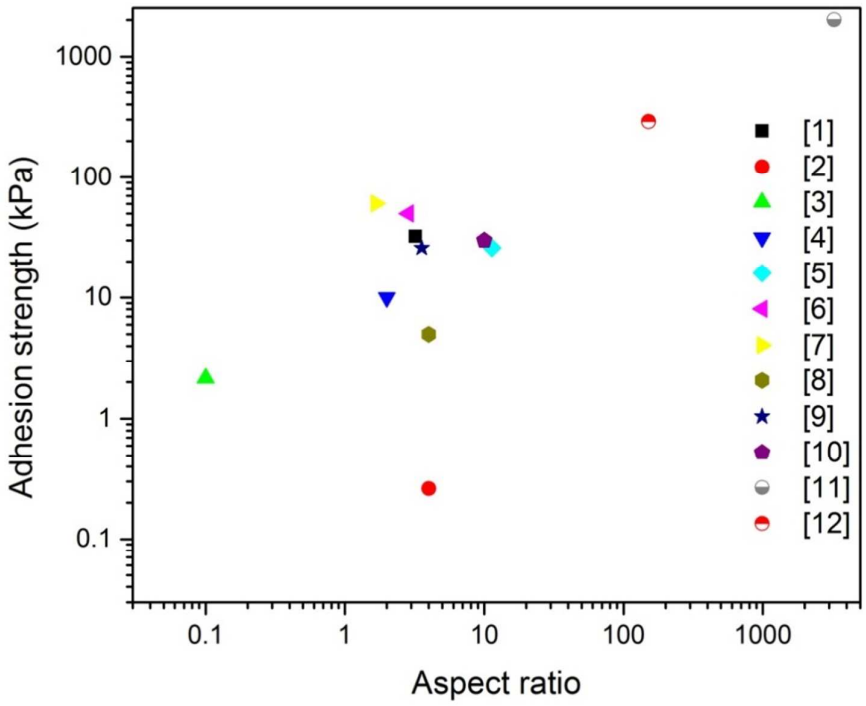

Figure 4

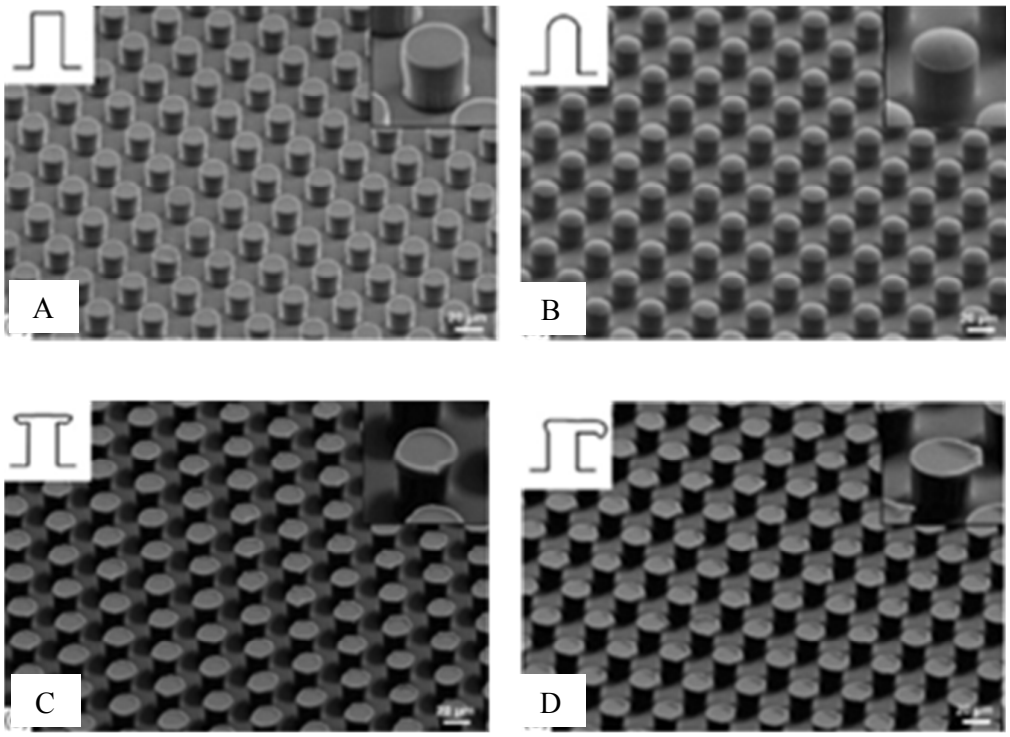

Figure 5

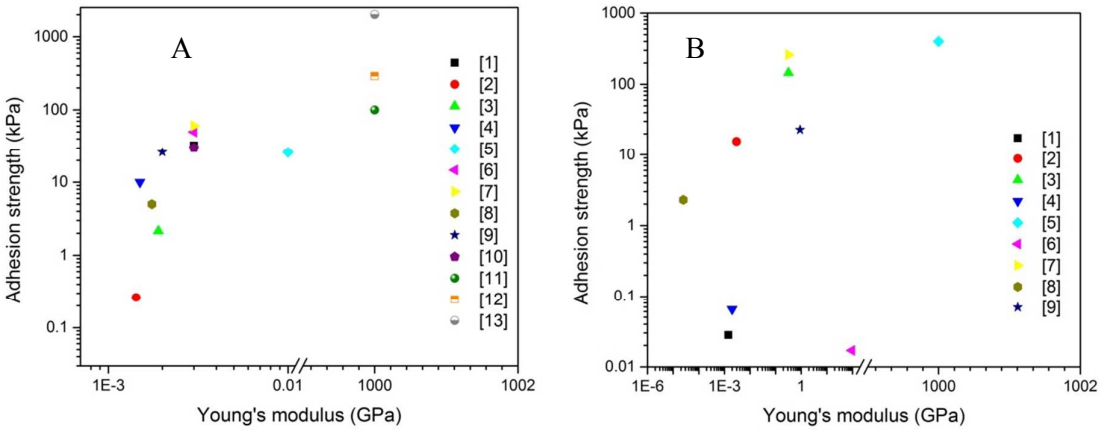

Figure 6

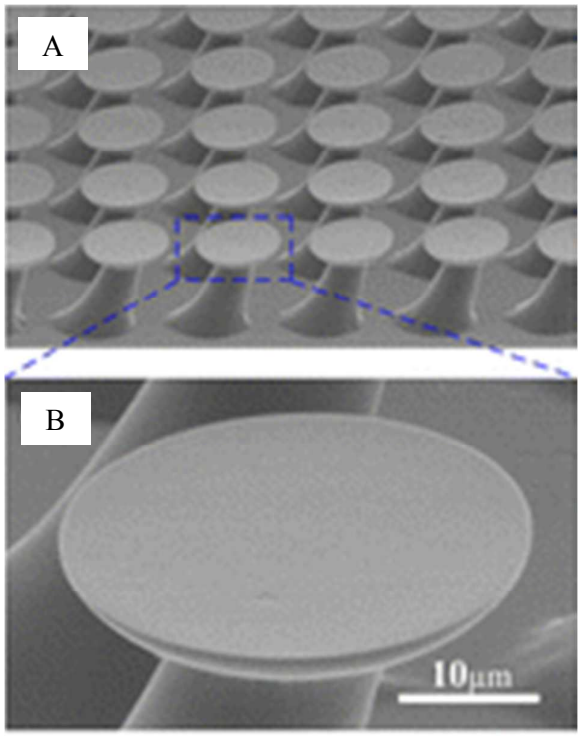

Figure 7

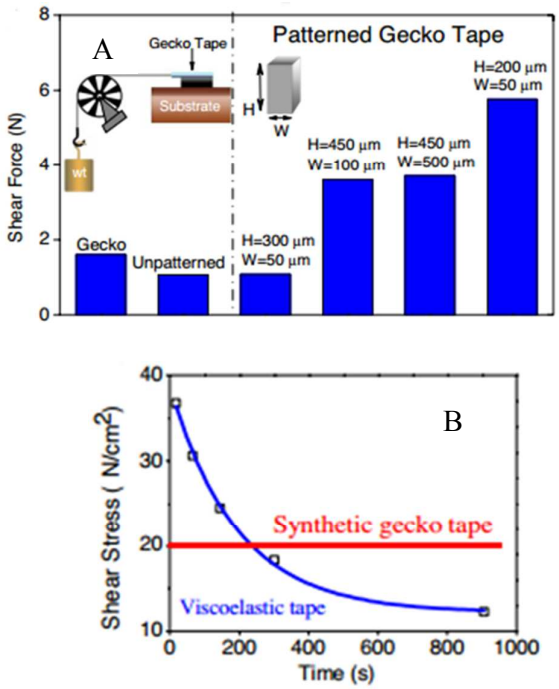

Figure 8

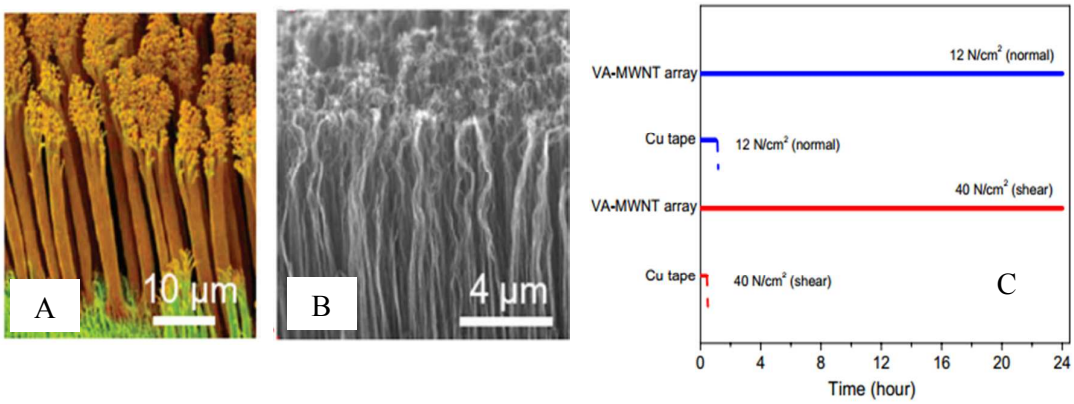

Figure 9